Cell Transplantation, Vol. 26, pp. 365–377, 2017

0963-6897/17 $90.00 + .00
DOI: https://doi.org/10.3727/096368916X693040
E-ISSN 1555-3892
www.cognizantcommunication.com

β-Catenin Accumulation Is Associated With Increased Expression of Nanog Protein and Predicts Maintenance of MSC Self-Renewal

Sang-Jin Yu,*[1,2] Hyun-Je Kim,*†[2] Eui Seok Lee,‡ Chung-Gyu Park,*§¶
Su Jin Cho,# and Soung-Hoo Jeon*§¶

*Department of Microbiology and Immunology, Seoul National University
College of Medicine, Seoul, Republic of Korea
†Department of Biomedical Sciences, Seoul National University
Graduate School, Seoul, Republic of Korea
‡Department of Oral and Maxillofacial Surgery, College of Medicine, Korea University,
Guro Hospital, Seoul, Republic of Korea
§Institute for Endemic Disease, Medical Research Center, Seoul National University
College of Medicine, Seoul, Republic of Korea
¶Translational Xenotransplantation Research Center, Seoul National University
College of Medicine, Seoul, Republic of Korea
#Department of Pediatrics, Ewha Womans University School of Medicine, Seoul, Republic of Korea

Human mesenchymal stem cells (hMSCs) are self-renewing cells with the ability to differentiate into organized, functional network of cells. Recent studies have revealed that activation of the Wnt/β-catenin pathway by a glycogen synthase kinase (GSK)-3-specific pharmacological inhibitor, Bio, results in the maintenance of self-renewal in both mouse and human ES cells. The molecular mechanism behind the maintenance of hMSCs by these factors, however, is not fully understood. We found that rEGF enhances the level of β-catenin, a component of the Wnt/β-catenin signaling pathway. Furthermore, it was found that β-catenin upregulates Nanog. EGF activates the β-catenin pathway via the Ras protein and also increased the Nanog protein and gene expression levels 2 h after rEGF treatment. These results suggest that adding EGF can enhance β-catenin and Nanog expression in MSCs and facilitate EGF-mediated maintenance of MSC self-renewal. EGF was shown to augment MSC proliferation while preserving early progenitors within MSC population and thus did not induce differentiation. Thus, EGF not only can be used to expand MSC in vitro but also be utilized to autologous transplantation of MSCs in vivo.

Key words: Human mesenchymal stem cells (hMSCs); Self-renewing cells; Epidermal growth factor (EGF); β-Catenin

INTRODUCTION

Mesenchymal stem cells (MSCs) are multipotent stromal cells that can differentiate into a variety of cell types such as adipocytes, chondrocytes, myocytes, and osteoblasts. Since the discovery and characterization of multipotent MSCs from bone marrow, MSC-like populations from other tissues have been characterized based on the "gold standard" criteria established for bone marrow-derived MSCs (BM-MSCs) (14,18,33,35). Recently, the Mesenchymal and Tissue Stem Cell Committee of the International Society for Cellular Therapy proposed three criteria to define MSCs (7,17). First, cells must be plastic adherent when maintained under standard culture conditions. Second, MSCs must express CD73, CD90, and CD105, and lack expression of CD34, CD45, CD14, CD11b, CD79, or CD19 and major histocompatibility complex (MHC) class II antigens. Third, MSCs must be able to differentiate into osteoblasts, adipocytes, and chondroblasts in vitro. MSCs have been recognized for their immunomodulatory properties (24,56), thus

Received December 29, 2015; final acceptance December 7, 2016. Online prepub date: September 27, 2016.
[1]Current affiliation: FOS Clinic, SM Tower (3rd Floor), 334 Gangnam-Daero, Gangnam-Gu, Seoul 135-936, Republic of Korea.
[2]These authors provided equal contribution to this work.
Address correspondence to Soung-Hoo Jeon, Ph.D., Department of Microbiology and Immunology, Institute of Endemic Disease, Medical Research Center, Xenotransplantation Research Center, Cancer Research Institute, Seoul National University College of Medicine, 103 Daehak-ro, Jongno-gu, 110-799 Seoul, Republic of Korea. Tel: +82-2-3668-7465; E-mail: shjeon1201@snu.ac.kr *or* Su Jin Cho, Department of Pediatrics, Ewha Womans University School of Medicine, 1071 Anyangcheon-ro, Yangcheon ku, Seoul, 158-710 Republic of Korea. E-mail: sujin-cho@ewha.ac.kr

broadening their potential for therapeutic use. However, the use of MSCs is limited by disadvantages such as oncogenicity (25,26,29,42,48,49), formation of ectopic unwanted tissue (3), unwanted release of cytokines, and replicative senescence after a few passages.

Recently there has been a series of publications on aggregation of MSCs either as a procedure for enhancing chrondrogenic differentiation of the cells (13,46,47) or to increase their therapeutic potential (20,21,39,51). Because aggregated human MSCs (hMSCs) were detected in the pulmonary microemboli after intravenous (IV) infusion of the cells (34,56), they tested the hypothesis that aggregation of hMSCs in culture may be effective in preactivating the cells to express tumor necrosis factor-inducible gene 6 (TSG-6) and thereby enhance their anti-inflammatory effects through a reduction in the lag period for expression of the gene in vivo.

Few trials in which MSCs are being administered to patients with type 1 diabetes (T1D) are ongoing. The first is a US-based trial on the use of allogeneic MSCs to determine safety and efficacy in patients affected by T1D (9). The use of stem cells (SCs) holds great promise for the cure of T1D due to their propitious immunological characteristics and their regenerative capabilities (8,9). MSCs showed multiple immunoregulatory properties in vitro and delayed allograft rejection in vivo when cotransplanted with islets (1). Hess et al. showed that bone marrow-derived c-kit$^+$ cells reduce hyperglycemia once adoptively transferred into chemically induced hyperglycemic mice. A low frequency of donor-derived insulin-positive cells was evident, and the majority of the transplanted cells were localized to ductal and islet structures, with stimulation of insulin production (16).

Epidermal growth factor (EGF) promotes formation of granulation tissue, stimulates fibroblast motility, and has been widely employed in studies to promote epidermal wound healing. MSCs are plastic-adherent cells with fibroblast-like morphology and have the capacity for multipotent differentiation in vitro (10). Wound healing mechanisms include differentiation of MSCs and paracrine effects of MSCs on epidermal and dermal cells (40,54). MSCs are known to have a strong paracrine capability of various growth factors and cytokines such as vascular endothelial growth factor (VEGF) or hepatocyte growth factor (HGF), which promote angiogenesis and wound healing (41). Thus, EGF can be used not only to expand MSCs in vitro but also to enhance cell dynamics and cell adhesion, which in turn promotes graft survival such as islet transplantation (1,16).

Nanog is a homeobox-containing transcription factor of approximately 280 amino acids. In the developing mouse embryo, Nanog plays a key role in determining the fate of the inner cell mass (ICM) cells, acting to sustain pluripotency and preventing differentiation (4). Nanog was identified as a factor that, when overexpressed, supported pluripotency even in the absence of a leukemia inhibitory factor (LIF)-based signal, and overexpression of Nanog without any other intervention is sufficient to sustain self-renewal. In the presence of fetal serum, activation of signal transducer and activator of transcription 3 (STAT3) by LIF is sufficient to maintain mouse embryonic stem cells (mESCs) in an undifferentiated state; however, this is not the case for human embryonic stem cells (hESCs) (6). Current literature suggest that Nanog is neither a target for STAT3 nor a regulator of STAT3 activity, but a direct downstream target for STAT3 in the maintenance of pluripotency (46).

Current literature suggests that Wnt/β-catenin signaling also has some role in the mESC self-renewal (47). The Wnt/β-catenin signaling pathway plays a crucial role in carcinogenesis as well as development. The embryonic processes it controls include body axis patterning, cell fate specification, cell proliferation, and cell migration. The action of Wnt is to maintain the intracellular levels of β-catenin, which then translocate to the nucleus where it forms a transcription complex with one of a number of transcription factors including T-cell factor (TCF) or lymphoid enhancer-binding factor 1 (LEF1). Tcf1 is found mainly in T lymphocytes, and Tcf4 is widely expressed and found in SCs of the gut, while Tcf3 is expressed in mESCs (31). The Wnt-controlled transcription factor Tcf3 has been shown to repress Nanog and thus promote differentiation.

Growth factors have become an important instrument in the attempt to control MSC differentiation properties. EGF acts by binding with high affinity to EGF receptor (EGFR) on the cell surface. This stimulates ligand-induced dimerization, activating the intrinsic protein tyrosine kinase activity of the receptor (15). The ERK activation by RasL61 or β-catenin was lowered by dominant negative Tcf4, indicating involvement of β-catenin/Tcf-mediated gene transcription in the ERK pathway regulation by Wnt/β-catenin signaling (20,34,55).

EGF has been shown to activate chondrogenic differentiation of MSCs. It remains unclear though whether preconditioning of MSCs by growth factors could result in deterioration of other properties.

With regard to their ongoing and increasing use in human subjects, we believe that a better understanding of how distinct variations of MSC culture conditions may alter their properties is essential. This will contribute to attempts at standardizing their handling and thus improve safety as well as comparability of scientific results. Therefore, the aim of this study was to determine effects of EGF supplementation during expansion of human BM-MSCs in two widely used cell culture media and the subsequent change of surface marker distribution and cell differentiation properties.

MATERIALS AND METHODS

Isolation and Expansion of hMSCs

The extracted human bone segments from the mandible were collected from three adults (18, 21, and 35 years of age). All patients provided written informed consent for the collection of samples and subsequent analysis. Institutional review board (IRB) approval was obtained, and all experiments have followed the principles outlined in the Declaration of Helsinki for all human or animal experimental investigations by the IRB of Korea University Guro-Hospital, Seoul, Republic of Korea (IRB No. KUGH09110).

The bone segments were digested in a solution of 3 mg/ml collagenase type I (Worthington Biochemical Corp., Lakewood, NJ, USA) and 4 mg/ml dispase (Boehringer Mannheim, Montreal, QC, Canada) for 1 h at 37°C. Single-cell suspensions were obtained by passing the cells through a 40-μm strainer (BD Falcon™; BD Biosciences, San Jose, CA, USA) and cultured on 100-mm-diameter uncoated culture plates (Corning Life Sciences, Tewksbury, MA, USA) in α-modification of Eagle's medium (Gibco BRL; Life Technologies, Grand Island, NY, USA) supplemented with 10% fetal calf serum (FCS; Gibco BRL), 100 μM ascorbic acid 2-phosphate (Wako Chemicals USA, Cape Charles, VA, USA), 2 mM glutamine (Sigma-Aldrich, St. Louis, MO, USA), 100 U/ml penicillin (Sigma-Aldrich), and 100 μg/ml streptomycin (Sigma-Aldrich) and then incubated at 37°C in 5% CO_2. All primary cells used in this study were at passage 3 or 11. The cells were divided every 4 days with 40% confluence.

The rabbit monoclonal antibody (RmAb) to human β-catenin was purchased from Cell Signaling Technology (Danvers, MA, USA); glyceraldehyde 3-phosphate dehydrogenase (GAPDH), phosphorylated STAT3 (pSTAT3), and STAT3 were purchased from Abcam (Cambridge, UK); Nanog was purchased from Santa Cruz Biotechnology (Santa Cruz, CA, USA); anti-Ras antibody, clone RAS10, was purchased from Merck Chemicals GmbH (Upstate, Darmstadt, Germany); stromal cell line antibody (STRO-1) was purchased from R&D Systems (Minneapolis, MN, USA); and the monoclonal anti-α-tubulin was purchased from Sigma-Aldrich. The antibodies for cytoskeleton (Alexa Fluor® 568 or 488 phalloidin) and fluorescence immunocytochemistry (Alexa Fluor 568 or 488) were purchased from Molecular Probes (Life Technologies Biotechnology Company, Eugene, OR, USA).

Flow Cytometry Analysis

The percentage of STRO-1^+ and $CD90^+$ cells was analyzed by flow cytometry; each cell stock at their second passage was seeded and cultured by the time the cells reached 90% of confluence. Approximately 1×10^6 cells were harvested using trypsin/ethylenediaminetetraacetic acid in phosphate-buffered saline (PBS) and cultured for 24 h to be stabilized. When the cells reached approximately 60% of confluence at their third passage, hMSCs were harvested from the culture dishes and fixed with 3.7% paraformaldehyde (PFA) for 1 min. The cells were blocked with 1% bovine serum albumin (BSA) for 2 h at 4°C and incubated with primary STRO-1 mAb (1 μg/ml) and CD90 mAb at 4°C for 30 min, and with secondary Alexa Fluor 488 antibody at room temperature (RT) for 30 min. The mixture of the cells was washed twice with PBS and fixed in 1% PFA. The negative control cells for each cell group were prepared the same as described above except for primary antibody incubation. Cells were analyzed using a FACSCalibur™ (BD Biosciences). A total of 10,000 viable cells were analyzed per sample, and the reading was repeated three times.

Three-Dimensional Culture System of hMSC and MSC Sphere Staining

To assess the aggregation ability, approximately 2.5×10^4 cells were seeded per 1 ml of α-minimum essential medium (MEM) media onto a 12-well culture plate and incubated overnight in 5% CO_2 at 37°C to be stable. The culture system is made of soft agar with different concentrations: a layer constituting the bottom is 1.6% agar and the top part where the cell layer is administered is composed of 0.8% agar. After 7 days of culture period, the microscopic images were captured using an Olympus CKX41 (Tokyo, Japan) microscopic digital camera and viewed using Adobe Photoshop 7.0 software (Adobe Systems Incorporated, San Jose, CA, USA). To aggregate hMSCs, we used a three-dimensional (3D) culture system. Phase-contrast microscopy showed the time course of the aggregation of 25,000 hMSCs into a spheroid in a hanging drop. The hMSC spheres were generated at their 3rd or 11th passage and cultured in a well of soft agar with or without EGF for 48 h at 37°C in 5% CO_2. Fixation was for 10 min at RT with 3.7% PFA in PBS at pH 7.4, and then permeabilization occurred for 3 min on ice with 0.1% Triton™ X-100 (Sigma-Aldrich) in PBS. The blocking procedure was performed with 1% BSA for 2 h at 4°C followed by washing in PBS (pH 7.4). Next, the hMSC spheres were incubated with stemness marker [Nanog, red (v/v); 1:200] (Santa Cruz Biotechnology Inc., Dallas, TX, USA) and surface marker [anti-human STRO-1, green (v/v); 1:200] (R&D Systems) for 2 h at RT. The spheres were subsequently incubated using secondary antibodies of Alexa Fluor 568 phalloidin and Alexa Fluor 488 (Life Technologies) for 30 min. Next the nuclei were stained in 4′,6-diamidino-2-phenylindole (DAPI; 1 μg/ml; Roche Applied Science, Pleasanton, CA, USA) for 5 min at RT. After washing with PBS several times, the slides were mounted in a mounting medium. The spheres were imaged using a confocal laser scanning microscope (LSM 510 META; Carl Zeiss, Heidenheim, Germany).

Immunoblot Analysis

For sodium dodecyl sulfate (SDS)-polyacrylamide gel electrophoresis (PAGE), the Laemmli buffer system (Sigma-Aldrich) was used to cast a 5% stacking gel and 10% resolving gel. After denaturation at 100°C for 3 min, proteins were resolved at a constant 20 mA in a Bio-Rad Mini-PROTEAN II apparatus (Bio-Rad Laboratories, Seattle, WA, USA) until the bromophenol blue reached the bottom of the gel. Anti-STAT3, anti-phospho-STAT3, anti-β-catenin, anti-Nanog, anti-Ras, anti-c-Myc, anti-GAPDH, and anti-α-tubulin primary antibodies were used, and then membranes were incubated with horseradish peroxidase (HRP)-conjugated secondary antibodies (Santa Cruz Biotechnology). Protein bands were observed by enhanced chemiluminescence using SuperSignal West Pico (Thermo Fisher Scientific, Schaumburg, IL, USA).

RT-PCR

The total RNA was prepared by TRIzol reagent (Invitrogen, Carlsbad, CA, USA) according to the manufacturer's protocol. The first-strand cDNA was synthesized through a cDNA synthesis kit (Invitrogen). The primer set for PCR included Nanog (sense, 5′-ATG AGT GTG GAT CCA GCT TG-3′; antisense, 5′-CTC CAG GTT GAA TTG TTC CA-3′). The PCRs were preincubated in a PCR Mastercycler gradient (Applied Biosystems, Carlsbad, CA, USA) at 95°C for 3 min and then cycled 33 times at 95°C for 30 s, 55°C for 30 s, and 72°C for 60 s, and then followed by a final 7-min extension at 72°C. The products were separated by electrophoresis on a 1% agarose gel and visualized by UV-induced fluorescence.

Real-Time Quantitative PCR

The hMSCs were plated in 100-mm culture dishes with α-MEM media and allowed to attach overnight in 5% CO_2 at 37°C. Total RNA was extracted from those cells using TRIzol® reagent (Invitrogen) according to the manufacturer's protocol. The concentration and purity of the RNA preparations were determined by measuring the absorbance of RNA at 230, 260, and 280 nm. The first-strand cDNA was synthesized using a first-strand cDNA synthesis kit (Invitrogen), and approximately 100–150 ng of total RNA was used for analysis. Real-time quantitative PCR was performed using EXPRESS SYBR GreenER™ SuperMix (Invitrogen) in a real-time PCR system (7500 Real-Time PCR System; Applied Biosystems). The primer set for PCR included Nanog (sense, 5′-T A C C C C A G C C T T T A C T C T T C-3′; antisense, 5′-C T C C A G G T T G A A T T G C A-3′). Measurements were performed in triplicate in a reverse transcription-negative blank of each sample, and a no-template blank served as negative controls. Amplification curves and gene expression were normalized to the housekeeping gene β-actin, which was used as an internal standard.

Immunocytochemical Staining

For immunocytochemical staining, cells (2×10^4 cells/well) were seeded on 22×22-mm coverslips in six-well plates. The cells were plated at their second passage and cultured for 24 h at 37°C in 5% CO_2. Fixation was for 10 min at RT with 3.7% PFA in PBS at pH 7.4, and then permeabilization occurred for 3 min on ice with 0.1% Triton™ X-100 (Sigma-Aldrich) in PBS. The blocking procedure was performed with 1% BSA for 2 h at 4°C followed by washing in PBS (pH 7.4). Next, the samples were incubated with primary mAbs (v/v, 1:200) for 2 h at RT. The cells were subsequently incubated using secondary antibodies of Alexa Fluor 488 and Alexa Fluor 568 phalloidin for 30 min. The nuclei were then stained in DAPI (1 μg/ml; Roche Applied Science) for 5 min at RT. After washing with PBS several times, the slides were mounted in a mounting medium. Cells were imaged using a confocal laser scanning microscope (LSM 510 META; Carl Zeiss).

Mineralization Induction

The hMSCs (8×10^4 cells/well) were seeded into six-well plates with normal growth media at their third passage. The media were changed to the mineralization induction media (α-MEM, 5 mM β-glycerol phosphate, and 10 nM dexamethasone) every 3 days. On day 21, accumulation of mineral nodules was detected by 2% Alizarin red S staining at pH 4.2 (Sigma-Aldrich) and observed with a light microscope (Olympus, Center Valley, PA, USA). The supernatant was quantified spectrophotometrically, and absorbance of samples was read at 562 nm.

RESULTS

EGF Is Involved in the Regulation of Aggregation of hMSCs Into Spheroids

Our previously published data have indicated that human alveolar BM-MSCs express markers such as STRO-1. We isolated hMSCs from alveolar bone according to previously described protocols (32). Most of the cells retained their fibroblastic spindle shape under light microscopic view (Fig. 1A). Adherent single-cell colonies were also shown (data not shown). Immunocytochemical staining with STRO-1 antibody showed that the majority of STRO-1 proteins were generally distributed in the cell-to-cell junctions (Fig. 1B). The fluorescence-activated cell sorting (FACS) analysis was performed with STRO-1. STRO-1 has been commonly used as a positive marker for hMSCs and was markedly expressed in hMSCs in this study. CD90 was suggested as one of the most reliable surface markers for hMSCs and has been confirmed in

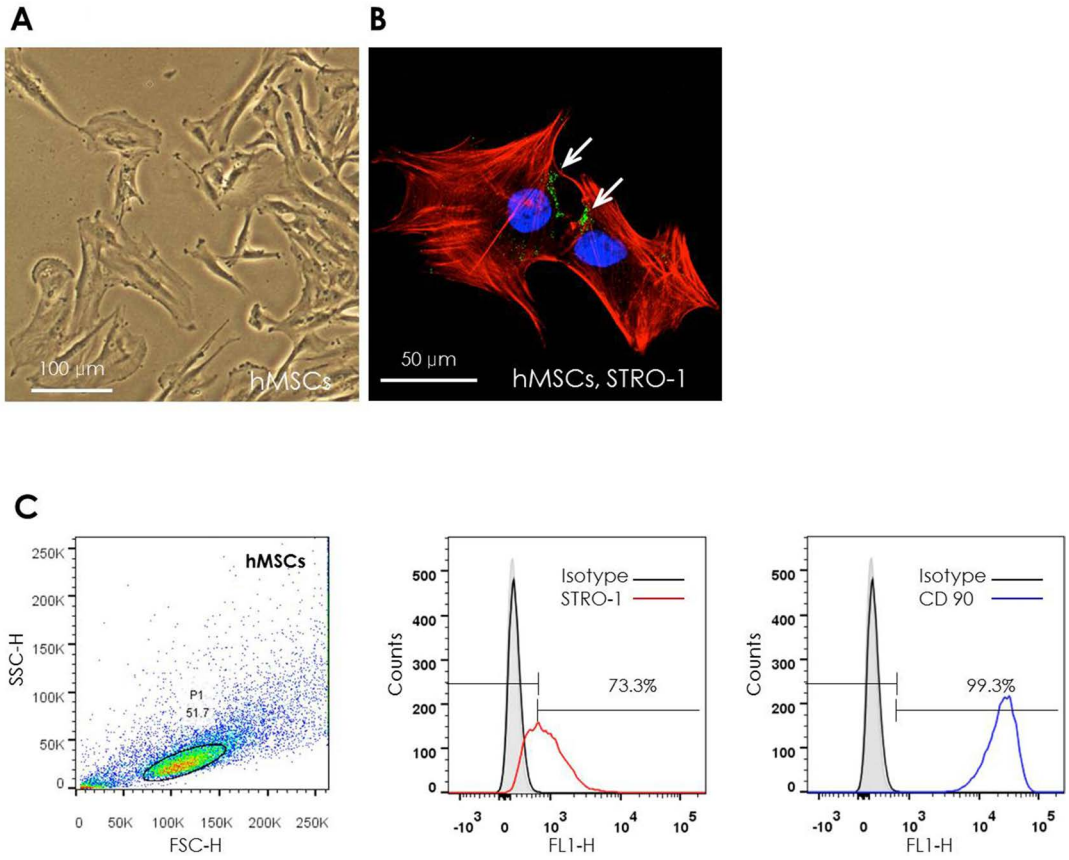

Figure 1. Characterization of human mesenchymal stem cells (hMSCs). (A) Light microscopic view of the adherent single-cell colony of hMSCs. Scale bar: 100 µm. (B) Immunocytochemical staining using STRO-1 as a mesenchymal stem cell marker. Cells were incubated with anti-STRO-1 antibody, followed by labeling with anti-mouse fluorescein isothiocyanate for STRO-1 (arrows). Cytoskeleton was visualized in red by labeling phalloidin with confocal microscope. 6-Diamidino-2-phenylindole (DAPI)-stained nuclei are shown in blue. Scale bar: 50 µm. (C) FACS analysis of hMSCs dissociated from primary cells of human bone segments and stained for STRO-1 and CD90. Cells were gated on viable cells (P1; left). In the histograms, STRO-1 and CD90 expression in hMSCs demonstrates an evident positivity; the black line indicates isotype cells. Percentages in each histogram are relative to total viable cells.

several studies as an intense marker for hMSCs (7,18,32). Thus, we started our study for human BM-MSCs focusing on cells with corresponding characteristics by flow cytometry (Fig. 1C). To aggregate hMSCs, we used a 3D culture (Fig. 2A). The microscopy demonstrated that hMSCs cultured in 3D culture system and gradually coalesced into a single central spheroid (Fig. 2B). After treatment of hMSCs with EGF, they increasingly incorporated into a central spheroid formation. This finding was consistent even after mineral induction. However, the aggregator of hMSCs disappeared dramatically when administered with the inhibitor of the EGF, cetuximab (Fig. 2B, top). The hMSCs were cultured in normal medium or mineralization induction medium. hMSCs not treated with EGF showed far more mineral nodules (crystal formation) compared to the cells with EGF treatment in the mineral induction medium (Fig. 2B, bottom). Confocal images show spheroid hMSCs stained with the indicated Nanog stemness marker (red). Anti-STRO-1 antibody (green) and DAPI staining (blue) are also shown (Fig. 2C). After treatment of hMSCs with EGF, Nanog was increasingly expressed into a spheroid (Fig. 2C). This result suggests that adding EGF can enhance cell aggregation and maintenance in hMSCs.

EGF Induces the Transcription Factor Nanog Turn On and Increases Protein Expression

We aimed to determine whether EGF affects hMSC differentiation properties via the STAT3 pathway. STAT3 activation is required for self-renewal of ESCs. Indeed LIF, which is supplied to murine ESC cultures to maintain their undifferentiated state, can be omitted if STAT3 is activated through some other means (27). Nanog was identified as a factor that when overexpressed supported pluripotency even in the absence of a LIF-based signal. In the embryo, Nanog expression is first seen at

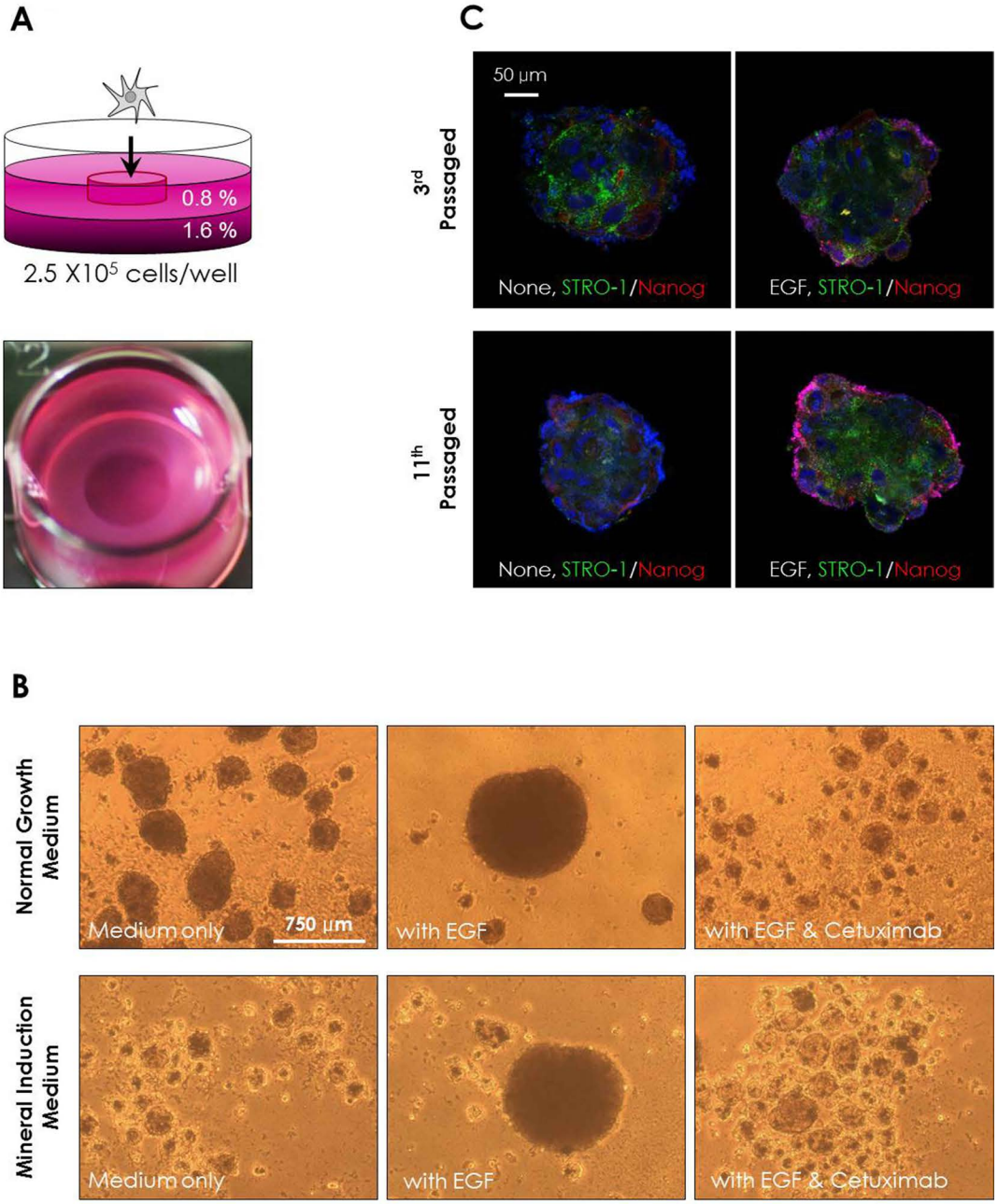

Figure 2. Design of 3D culture system and spheroid hMSCs. (A) The 3D culture system for hMSCs. The culture system is made of soft agar, a layer constituting the bottom is 1.6% agar, to administration of the cell layer was composed of 0.8% agar. The 12-well plate was used, and cells were seeded 2.5×10^4 per well. (B) Phase-contrast microscopy showing the aggregation of 250,000 hMSCs into a spheroid in a hanging drop. Cells were grown in α-modification of Eagle's medium (α-MEM) with or without 20 ng/ml EGF and/or cetuximab for 7 days before image capture. Scale bar: 750 μm. (C) Confocal images of spheroid hMSCs stained with the indicated Nanog stemness marker (red). Anti-STRO-1 antibody (green) and DAPI staining (blue) are also shown. Scale bar: 50 μm.

the compacted morulae stage before becoming restricted to the ICM, the postimplantation stage when Nanog expression is drastically reduced. In vitro, Nanog expression is robust in the pluripotent cell types but is absent from adult tissues (4). The LIF was among one of the earliest molecules found to be associated with the maintenance of SC self-renewal in vitro and in vivo.

We measured the effect of pSTAT3 and STAT3 protein expression or Nanog on immunoblot and RT-PCR stimulated by LIF and/or EGF (Fig. 3A–D). LIF treatment

increased the intensity of STAT3 protein in the 3rd passaged and 11th passaged hMSCs. However, treatment of EGF with LIF or without LIF did not affect the STAT3 protein expression, and also the pSTAT3 was increased in the EGF-treated 3rd passaged and 11th passaged hMSCs (Fig. 3A).

The Wnt signaling pathways regulate satellite cell self-renewal and myogenesis during embryogenesis (13). ERK pathway regulation by β-catenin occurs at least partly via cross-talk of the Ras protein (20). Studies have shown that β-catenin is able to upregulate octamer-binding transcription factor 4 (Oct4) expression and interact with Nanog and thus promote self-renewal (47).

To determine whether EGF affects Nanog expression via the β-catenin pathway, we examined the effect of Ras, pErk, pSTAT3, β-catenin, and Nanog expression on hMSCs by EGF using immunoblot. Ras, pErk, pSTAT3, β-catenin, and Nanog protein levels were increased by

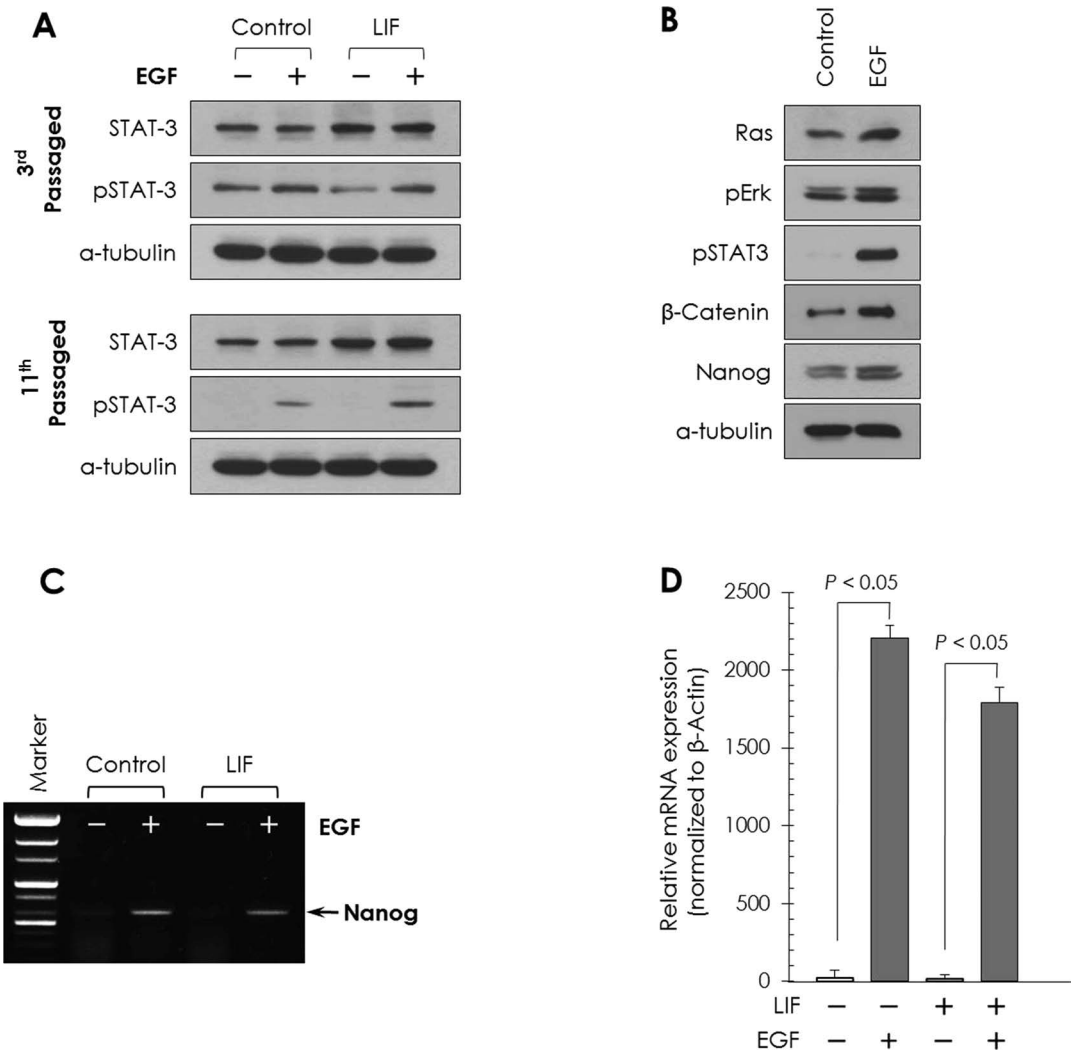

Figure 3. (A) Immunoblot showing the effects of EGF and/or leukemia inhibitor factor (LIF). EGF was treated 20 ng/ml for 2 h. Cell extracts were resolved on 10% sodium dodecyl sulfate-polyacrylamide gel electrophoresis (SDS-PAGE) from 3rd or 11th passaged cells, respectively, and STAT3 and pSTAT3 proteins were detected by immunoblot analysis as described in the Materials and Methods section. α-Tubulin was used as a loading control. (B) Immunoblot showing the effects of EGF. Cells were grown in α-MEM with or without 20 ng/ml EGF for 2 h before harvesting. Immunoblot analysis was performed on cell lysates for the detection of Ras, pErk, pSTAT3, β-catenin, Nanog, and α-tubulin. (C) Reverse transcriptase polymerase chain reaction (RT-PCR) analysis of hMSCs. The PCR shows the presence of 620-bp bands in human Nanog. (D) The relative mRNA expression of Nanog normalized to β-actin was remarkably increased in EGF compared with the control group. The mRNA expression of Nanog was not increased in LIF-treated hMSCs, but the EGF/LIF treatment group was increased. Data are means ± SD from $n = 3$ independent experiments. The p values were determined by unpaired two-tailed Student's t-test.

inoculation of EGF (Fig. 3B). The EGF-treated hMSCs turned on the gene expression of Nanog by PCR (Fig. 3C). To investigate whether the EGF-induced stemness was accompanied by an increase in the Nanog gene expressions, we performed real-time quantitative PCR. The relative mRNA expression of Nanog was remarkably increased in EGF-treated hMSCs compared with the hMSCs not treated with EGF, while the expression of Nanog was highly increased in EGF-treated hMSCs, but the amount was less than the increase in EGF/LIF-treated hMSCs (Fig. 3D). The only genes expressed more than 153-fold in EGF-only-treated cells and 120-fold in EGF/LEF-treated cells were Nanog (Fig. 3D).

To identify the involvement of EGF in hMSC stemness, we measured the effects of EGF (Fig. 3B). The Ras, pErk, pSTAT3, β-catenin, and Nanog levels, which were increased by 2 h of stimulation with EGF in hMSCs, indicate the functionality of EGF. Interestingly, we noticed an increase in nonphosphorylated Ras, β-catenin, and Nanog by immediate EGF signaling (Fig. 3B). Notably, we also observed reductions of β-catenin, pSTAT3, and Nanog by the β-catenin inhibitor PNU-74654 (Fig. 5D), which indicates specificity in the regulation of the stemness and ERK pathway components in hMSCs by EGF. Therefore, EGF activates the β-catenin pathway via Ras protein and also increased the amount of Nanog protein and gene expression levels at 2 h after EGF treatment. This result suggests that EGF can increase Nanog expression via the β-catenin pathway and can enhance maintenance of hMSCs (Figs. 2B and C and 3B).

We also investigated the effect of EGF induction on β-catenin and Nanog protein by immunocytochemical analysis. β-Catenin and Nanog protein overexpressed by the addition of EGF were mostly localized in the nucleus area of hMSCs compared to control groups (Fig. 4A and B). β-Catenin remained in the perinuclear area of cells and increased movement into the nucleus by inoculation of EGF at 2 h (Fig. 4A). Nuclear Nanog protein was activated by EGF at 2 h (Fig. 4B).

To measure the expression of β-catenin and Nanog protein in hMSCs as maintained by EGF, we used FACS (Fig. 4C). Cells were gated on the quantity of viable cells. Autofluorescence was detected for Nanog (PE-A channel) and β-catenin (FITC-A channel). In the histograms, Nanog and β-catenin expression in hMSCs demonstrates an evident positivity; the black line indicates isotype cells. Percentages denoting expression levels are shown in each histogram, which compare controls to the EGF-treated cells. The β-catenin and Nanog had a protein expression of 93.96% and 95.65%, respectively, in hMSCs (Fig. 4C). These results suggest that adding EGF can enhance β-catenin and Nanog expression in EGF-mediated maintenance of hMSC self-renewal.

EGF Inhibits Mineralization via the β-Catenin Pathway in hMSCs

To assess whether EGF contributes to mineralization of hMSCs, we treated the hMSCs with human recombinant EGF (rEGF). The effect of rEGF-induced mineralization was confirmed by Alizarin red staining (Fig. 5A). Mineralization of the hMSCs was compared without rEGF (control: with PBS) or with rEGF (experimental) under normal growth or mineralization induction condition. The Alizarin red-stained samples underwent destaining procedure, incubating the samples at RT for 15 min with 3 ml of 10 mM sodium phosphate 10% acetyl pyrimidium (pH 7.0) solution. The calcium content measured from the destained samples followed the same trend as the results of Alizarin red-stained samples. The destained samples were then transferred to a 96-well plate, and the absorbance was measured at 562 nm (Fig. 5B). The mineralization results after 3 weeks demonstrate that the hMSCs cultured at 1 mg/ml calcium hydroxide concentration under the mineralization induction media have far higher mineralization reaction than under the normal growth media. However, the cells treated with rEGF and cultured under normal growth media did not show mineralization. The hMSCs cultured with cetuximab under mineralization induction media showed increased calcium content despite rEGF treatment, whereas the cells cultured under normal growth media showed no increase in calcium (Fig. 5A and B).

To identify involvement of EGF in the regulation of the β-catenin pathway, we measured the level of β-catenin after 20 ng/ml rEGF treatment of hMSCs for 2 h. Immunoblots showed increased β-catenin levels. The level of Nanog was also increased with increased pSTAT3 and β-catenin, whereas treatment with cetuximab decreased it (Fig. 5C). EGF stimulation and sequential increase in pSTAT3 activated the β-catenin signaling pathway, and the increase in Nanog induced self-renewal of hMSCs. In addition, experiments using PNU-74654 to inhibit β-catenin exhibited the same effect as that of the addition of cetuximab (Fig. 5D). The results indicate that rEGF is a major factor for increasing the expression of Nanog via the β-catenin pathway in hMSCs.

DISCUSSION

Pluripotent SCs may be isolated from the embryonic ICM and expanded. However, most of the tissues of an adult organism generally include a small pool of cells (adult SCs) with an inherent ability to maintain the pool through self-replication and produce more dedicated progenitor cells through multiple lineage differentiation (53).

hMSCs remain one of the most promising tools for use in regenerative medicine due to their multilineage

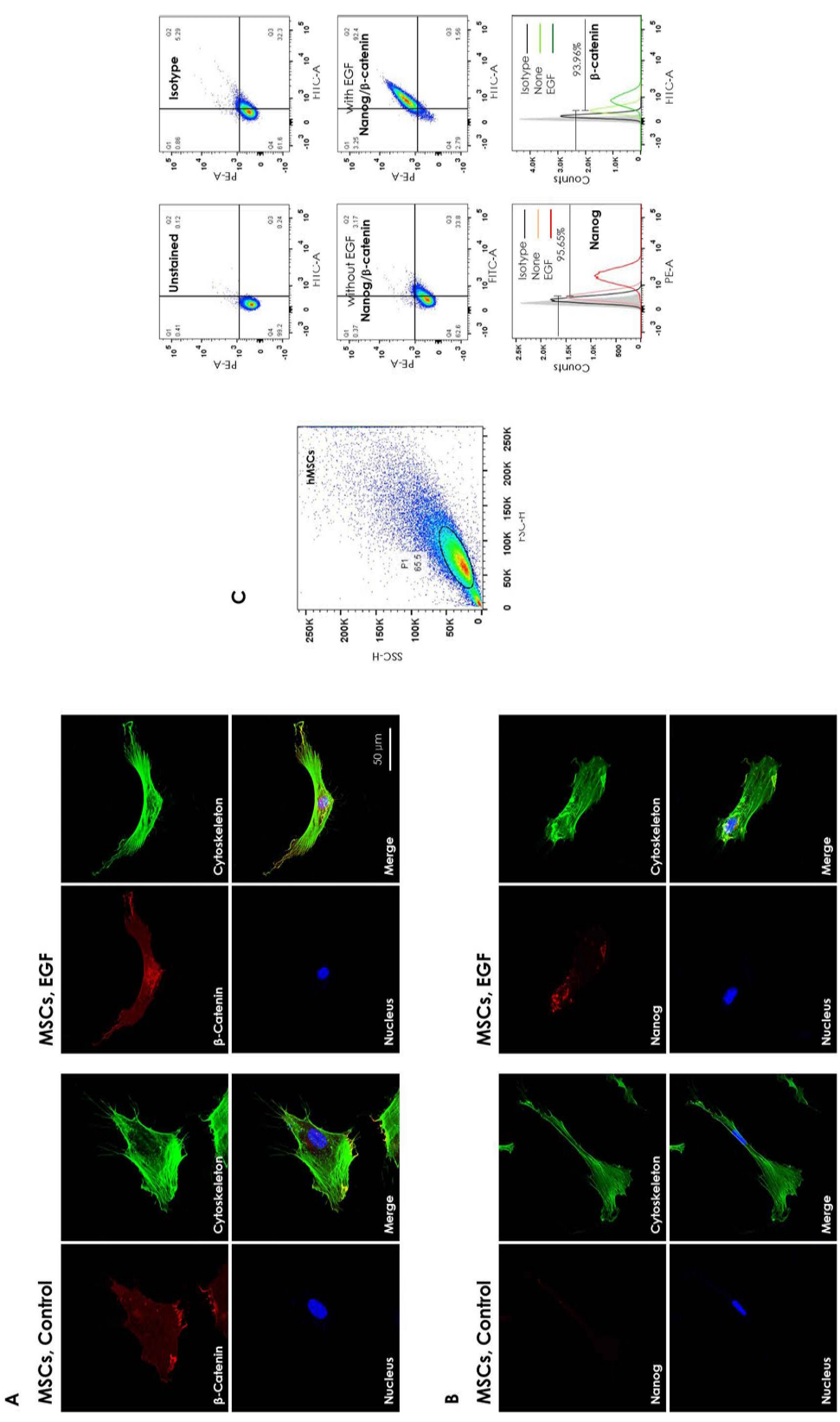

Figure 4. Effect of EGF in human mesenchymal stem cells. (A, B) Immunocytochemical analysis of β-catenin or Nanog by EGF. The hMSCs were grown in α-MEM and added with 20 ng/ml EGF for 2 h. Cells were incubated with anti-β-catenin or anti-Nanog antibodies followed by labeling with anti-mouse rhodamine for β-catenin or Nanog detection. Cytoskeleton was visualized in green by labeling phalloidin with confocal microscope. Cell nuclei were stained with DAPI. Scale bar: 50 μm. (C) FACS analysis of hMSCs dissociated from primary cells of human bone segments and stained for Nanog and β-catenin. Cells were gated on viable cells (P1; left). Autofluorescence was detected in Nanog (PE-A channel) and β-catenin (FITC-A channel). In the histograms, Nanog and β-catenin expression in hMSCs demonstrates an evident positivity; the black line indicates isotype cells. Percentages in each histogram are relative to EGF-treated cells.

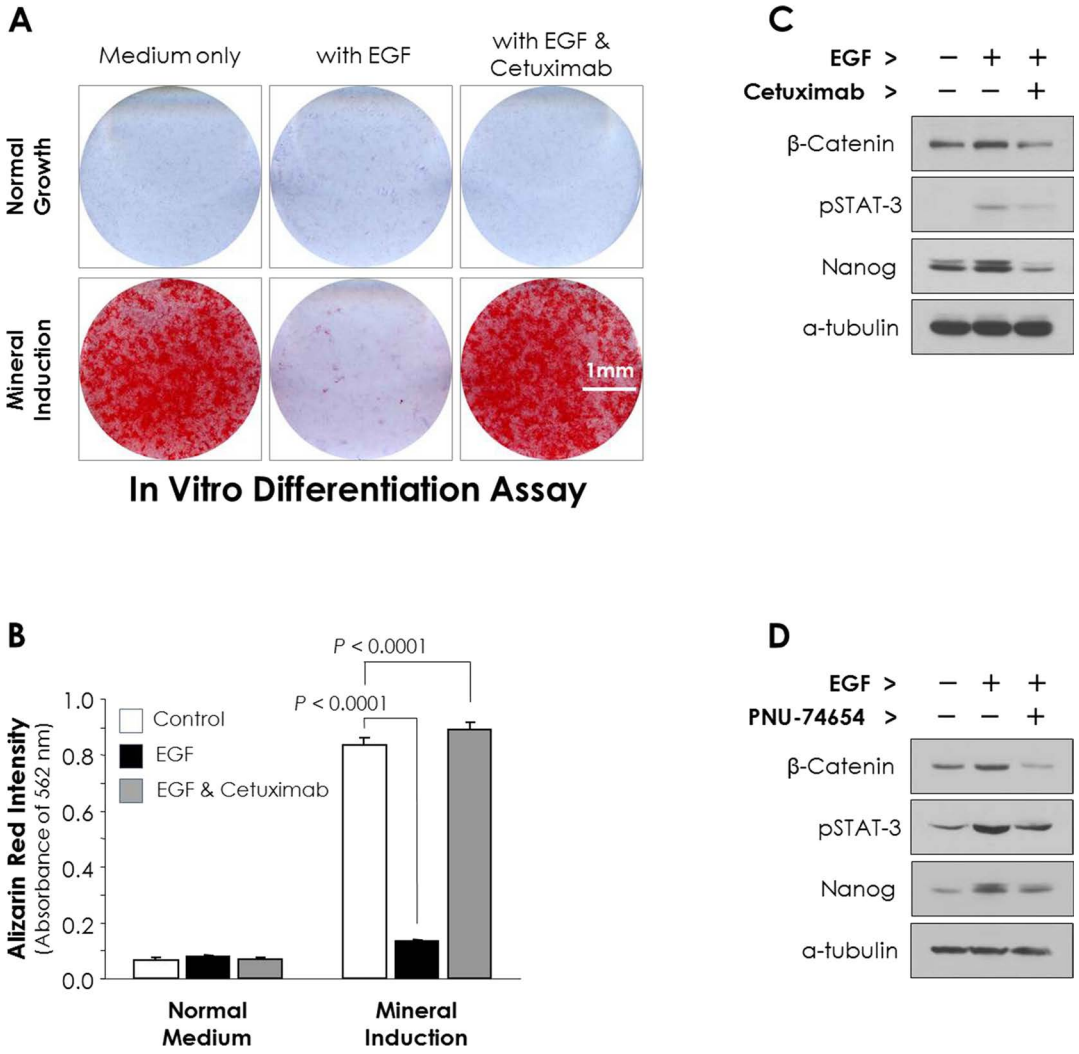

Figure 5. Effects of mineralization on the hMSCs with EGF and/or cetuximab. (A) The hMSCs were grown in α-MEM, and mineralization was induced with β-glycerophosphate and dexamethasone. Alizarin red staining shows mineral nodule formation with induction as described in the Materials and Methods section. Note the significant mineralized nodules in the induction media with cetuximab but no mineral nodule formation with EGF. Scale bar: 1 mm. (B) The Alizarin red-stained samples were destained as described in the Materials and Methods section, and the absorbance was measured at 562 nm. Data are means ± SD from $n = 3$ independent experiments. The p values were determined by unpaired two-tailed Student's t-test. (C) Immunoblot analysis was performed to detect β-catenin, pSTAT3, Nanog, and α-tubulin. EGF at 20 ng/ml and/or cetuximab was added to cells 2 h before harvesting. (D) EGF at 20 ng/ml and/or the β-catenin inhibitor PNU-74654 at 2 μg/ml was added to cells 2 h before harvesting.

potential. However, recent findings suggest that they are a heterogeneous population with differentiation potential (38,50). As culture conditions vary enormously between different laboratories, this may result in culturing different cell populations in different places, although all of them are referred to as MSCs. Even after obtaining the clinical characteristics of hMSCs, the cultured MSCs can be induced to differentiate under experimental cell culture conditions in the laboratory(21,39,51).

According to previous reports, human bone marrow cells include postnatal SCs that carry the ability to differentiate into osteoblasts, adipocytes, and neuron-like cells. Such SCs were STRO-1/CD146$^+$ progenitors derived from the perivascular area of the bone marrow (43). In this study, we isolated and antigenically defined the adult hMSCs as a population of SCs with early characteristics that are comparable to STRO-1 cells (Fig. 1A–C).

The cell culture conditions, such as the addition of specific cell growth factors, influence the proliferation and differentiation of hMSCs. The most commonly used growth factors are basic fibroblast growth factor (bFGF), transforming growth factor-β (TGF-β), and platelet-derived growth factor (PDGF), which could replace the serum component in cell culture medium to expand

hMSCs ex vivo without compromising differentiation potential (2,30,52). A report found that soluble EGF was shown to augment MSC proliferation while preserving early progenitors within the MSC population and thus did not induce differentiation (23). This is similar to the findings observed previously with large hMSC spheroids (36) and hMSCs in 3D culture (11).

MSCs have a significant immunoregulatory function, both toward developing thymocytes (45) and peptide-specific mature T cells (22), which might play a role in tumor–T cell interaction during neoplastic growth.

We applied human rEGF at the beginning of one passage to ensure that cell preparations were composed of homogeneous hMSCs. If we treat MSCs with soluble EGF or rEGF in vitro, there is no risk of tumor formation because the half-life of the EGF limits tumorigenic effects. We also needed to determine whether administration of rEGF had any influence on hMSCs when applied to cells that had been cultured with rEGF and/or cetuximab for 11 passages (Fig. 3A).

Cetuximab is an EGFR inhibitor used for the treatment of metastatic colorectal cancer and metastatic non-small cell lung cancer. When growth factors bind to their receptors on the surface of the cell, the receptors give a signal that causes cells to divide. Cetuximab binds to such receptors and turns off that signal (28). The microscopy demonstrated that hMSCs cultured in wells first formed numerous small aggregates that gradually combined into a single central spheroid along the lower surface of the wells. However, the spheroid did not increase as aggregates with cetuximab in normal growth and mineral-induced media (Fig. 2B). These findings are supported by our own data, clearly indicating acceleration of aggregation from the beginning of rEGF administration and improved maintenance of hMSCs.

Wnt signaling plays an essential role in embryonic development and also in the maintenance of adult SCs in various tissues. In the canonical Wnt pathway, acting via β-catenin and Tcf/Lef factors (12,44), β-catenin is a well-known cytoplasmic protein and has a role in cell–cell adhesion, acting to link membrane-bound cadherin to the actin elements in the cytoskeleton and also acting as a signaling molecule inside cells as part of the canonical Wnt signaling pathway (37). It has recently been shown that β-catenin is able to upregulate Oct4 expression and interact with Nanog and thus promote self-renewal (47); inhibition of Nanog results in increased differentiation. Nanog genes are essential for the development and pluripotency of various tissues as well as fate determination in SCs (5,19).

Our study reveals that genetic analysis such as RT-PCR in hMSCs has shown increased levels of mRNA for self-renewal markers, such as Nanog, that was also confirmed at the protein level using immunofluorescence staining and immunoblot (Fig. 3A and B) and also reveals that rEGF had a significant influence on other important signaling molecules, such as expression of Ras, β-catenin, and Nanog (Fig. 3C).

The differentiation potential of hMSCs was confirmed by mineralization induction. Mineralization induction for 3 weeks led the hMSCs to make mineral nodules, which was confirmed by Alizarin red staining. In this study, Alizarin red staining was used to find out the effect of calcium hydroxide on the mineralization of hMSCs. More of the small round Alizarin red-positive nodules were found in the cells grown in the culture with mineralization induction media, and this tendency was more evident even to the naked eye when the mineralization induction media were used compared with the normal growth media, and an increase in Alizarin red-positive nodules with cetuximab in mineral-induced media was noted as well. However, the Alizarin red-positive nodules did not increase as with rEGF in normal growth and mineral-induced media (Fig. 5A). To analyze such data quantitatively, the absorbance was measured at 562 nm. As a result, it was evident that calcium accumulation had comparatively increased in the cells grown in the mineralization induction media or with cetuximab than in the normal growth media or with rEGF (Fig. 5B).

To summarize the results, it was biochemically and physiologically evident that rEGF decreased the cell differentiation potential of the hMSCs. Such a result is valuable for the in vitro cultivation of the hMSCs. Future studies must focus on the molecular and cellular changes playing an important role in dedifferentiation, physiology/embryology, treatment-related procedures, and SC-related therapies, which will contribute to a better transplantation practice.

ACKNOWLEDGMENTS: This work was supported by the grants from the National Research Foundation of Korea (NRF) funded by the Basic Science Research Program through the Ministry of Education, Science and Technology (NRF-2011-0011716) to Soung-Hoo Jeon. This research was supported by a grant from the Korea Health Technology R&D Project through the Korea Health Industry Development Institute (KHIDI), funded by the Ministry of Health & Welfare, Republic of Korea (Grant No. HI13C0954). This study was supported by intramural research promotion grants from Ewha Womans University School of Medicine. The authors have no other relevant affiliations or financial involvement with any organization or entity with a financial interest in or financial conflict with the subject matter or materials discussed in the manuscript apart from those disclosed. No writing assistance was utilized in the production of this manuscript.

REFERENCES

1. Ben Nasr, M.; Vergani, A.; Avruch, J.; Liu, L.; Kefaloyianni, E.; D'Addio, F.; Tezza, S.; Corradi, D.; Bassi, R.; Valderrama-Vasquez, A.; Usuelli, V.; Kim, J.; Azzi, J.; Essawy, B. E.; Markmann, J.; Abdi, R.; Fiorina, P. Co-transplantation of autologous MSCs delays islet allograft rejection and

generates a local immunoprivileged site. Acta Diabetol. 52:917–927; 2015.
2. Bernardo, M. E.; Pagliara, D.; Locatelli, F. Mesenchymal stromal cell therapy: A revolution in regenerative medicine? Bone Marrow Transplant. 47:164–171; 2012.
3. Breitbach, M.; Bostani, T.; Roell, W.; Xia, Y.; Dewald, O.; Nygren, J. M.; Fries, J. W.; Tiemann, K.; Bohlen, H.; Hescheler, J.; Welz, A.; Bloch, W.; Jacobsen, S. E.; Fleischmann, B. K. Potential risks of bone marrow cell transplantation into infarcted hearts. Blood 110:1362–1369; 2007.
4. Chambers, I.; Colby, D.; Robertson, M.; Nichols, J.; Lee, S.; Tweedie, S.; Smith, A. Functional expression cloning of Nanog, a pluripotency sustaining factor in embryonic stem cells. Cell 113:643–655; 2003.
5. Chambers, I.; Silva, J.; Colby, D.; Nichols, J.; Nijmeijer, B.; Robertson, M.; Vrana, J.; Jones, K.; Grotewold, L.; Smith, A. Nanog safeguards pluripotency and mediates germline development. Nature 450:1230–1234; 2007.
6. Dahéron, L.; Opitz, S. L.; Zaehres, H.; Lensch, M. W.; Lensch, W. M.; Andrews, P. W.; Itskovitz-Eldor, J.; and Daley, G. Q. LIF/STAT3 signaling fails to maintain self-renewal of human embryonic stem cells. Stem Cells 22: 770–778; 2004.
7. Dominici, M.; Le Blanc, K.; Mueller, I. Slaper-Cortenbach, I.; Marini, F.; Krause, D.; Deans, R.; Keating, A.; Prockop, D. J.; Horwitz, E. Minimal criteria for defining multipotent mesenchymal stromal cells. The International Society for Cellular Therapy position statement. Cytotherapy 8:315–317; 2006.
8. Fiorina, P.; Jurewicz, M.; Augello, A.; Vergani, A.; Dada, S.; La Rosa, S.; Selig, M.; Godwin, J.; Law, K.; Placidi, C.; Smith, R. N.; Capella, C.; Rodig, S.; Adra, C. N.; Atkinson, M.; Sayegh, M. H.; Abdi, R. Immunomodulatory function of bone marrow-derived mesenchymal stem cells in experimental autoimmune type 1 diabetes. J. Immunol. 183:993–1004; 2009.
9. Fiorina, P.; Voltarelli, J.; and Zavazava, N. Immunological applications of stem cells in type 1 diabetes. Endocr. Rev. 32(6):725–754; 2011.
10. Friedenstein, A. J.; Gorskaja, J. F.; Kulagina, N. N. Fibroblast precursors in normal and irradiated mouse hematopoietic organs. Exp. Hematol. 4:267–274; 1976.
11. Frith, J. E.; Thomson, B.; Genever, P. Dynamic three-dimensional culture methods enhance mesenchymal stem cell properties and increase therapeutic potential. Tissue Eng. Part C Methods 16:735–749; 2010.
12. Fujimaki, S.; Hidaka, R.; Asashima, M.; Takemasa, T.; Kuwabara, T. Wnt protein-mediated satellite cell conversion in adult and aged mice following voluntary wheel running. J. Biol. Chem. 289:7399–7412; 2014.
13. Fujimaki, S.; Machida, M.; Hidaka, R.; Asashima, M.; Takemasa, T.; Kuwabara, T. Intrinsic ability of adult stem cell in skeletal muscle: An effective and replenishable resource to the establishment of pluripotent stem cells. Stem Cells Int. 2013:420164; 2013.
14. Gronthos, S.; Zannettino, A. C.; Hay, S. J.; Shi, S.; Graves, S. E.; Kortesidis, A.; Simmons, P. J. Molecular and cellular characterisation of highly purified stromal stem cells derived from human bone marrow. J. Cell Sci. 116:1827–1835; 2003.
15. Herbst, R. S. Review of epidermal growth factor receptor biology. Int. J. Radiat. Oncol. Biol. Phys. 59:21–26; 2004.
16. Hess, D.; Li, L.; Martin, M.; Sakano, S.; Hill, D.; Strutt, B.; Thyssen, S.; Gray, D. A.; Bhatia, M. Bone marrow-derived stem cells initiate pancreatic regeneration. Nat. Biotechnol. 21:763–770; 2003.
17. Horwitz, E. M.; Le Blanc, K.; Dominici, M.; Mueller, I.; Slaper-Cortenbach, I.; Marini, F. C.; Deans, R. J.; Krause, D. S.; Keating, A. Clarification of the nomenclature for MSC: The International Society for Cellular Therapy position statement. Cytotherapy 7:393–395; 2005.
18. Hung, S. C.; Chen, N. J.; Hsieh, S. L.; Li, H.; Ma, H. L.; Lo, W. H. Isolation and characterization of size-sieved stem cells from human bone marrow. Stem Cells 20:249–258; 2002.
19. Ivanova, N.; Dobrin, R.; Lu, R.; Kotenko, I.; Levorse, J.; DeCoste, C.; Schafer, X.; Lun, Y.; Lemischka, I. R. Dissecting self-renewal in stem cells with RNA interference. Nature 442:533–538; 2006.
20. Jeon, S. H.; Yoon, J. Y.; Park, Y. N.; Jeong, W. J.; Kim, S.; Jho, E. H.; Surh, Y. J.; Choi, K. Y. Axin inhibits extracellular signal-regulated kinase pathway by Ras degradation via beta-catenin. J. Biol. Chem. 282:14482–14492; 2007.
21. Jiang, Y.; Jahagirdar, B. N.; Reinhardt, R. L.; Schwartz, R. E.; Keene, C. D.; Ortiz-Gonzalez, X. R.; Reyes, M.; Lenvik, T.; Lund, T.; Blackstad, M.; Du, J.; Aldrich, S.; Lisberg, A.; Low, W. C.; Largaespada, D. A.; Verfaillie, C. M. Pluripotency of mesenchymal stem cells derived from adult marrow. Nature 418:41–49; 2002.
22. Krampera, M.; Glennie, S.; Laylor, R.; Simpson, E.; Dazzi, F. Bone marrow mesenchymal stem cells inhibit the response of naïve and memory antigen-specific T cells to their cognate peptide. Blood 101:3722–3729; 2003.
23. Krampera, M.; Pasini, A.; Rigo, A.; Scupoli, M. T.; Tecchio, C.; Malpeli, G.; Scarpa, A.; Dazzi, F.; Pizzolo. G.; Vinante, F. HB-EGF/HER-1 signaling in bone marrow mesenchymal stem cells: Inducing cell expansion and reversibly preventing multilineage differentiation. Blood 106:59–66; 2005.
24. Le Blanc, K.; Ringden, O. Immunomodulation by mesenchymal stem cells and clinical experience. J. Intern. Med. 262:509–525; 2007.
25. Li, H.; Fan, X.; Kovi, R. C.; Jo, Y.; Moquin, B.; Konz, R.; Stoicov, C.; Kurt-Jones, E.; Grossman, S. R.; Lyle, S.; Rogers, A. B.; Montrose, M.; Houghton, J. Spontaneous expression of embryonic factors and p53 point mutations in aged mesenchymal stem cells: A model of age-related tumorigenesis in mice. Cancer Res. 67:10889–10898; 2007.
26. Li, N.; Yang, R.; Zhang, W.; Dorfman, H.; Rao, P.; Gorlick, R. Genetically transforming human mesenchymal stem cells to sarcomas: Changes in cellular phenotype and multilineage differentiation potential. Cancer 115:4795–4806; 2009.
27. Matsuda, T.; Nakamura, T.; Nakao, K.; Arai, T.; Katsuki, M.; Heike, T.; Yokota, T. STAT3 activation is sufficient to maintain an undifferentiated state of mouse embryonic stem cells. EMBO J.18:4261–4269; 1999.
28. Messersmith, W. A.; Ahnen, D. J. Targeting EGFR in colorectal cancer. N. Engl. J. Med. 359:1834–1836; 2008.
29. Miura, M.; Miura, Y.; Padilla-Nash, H. M.; Molinolo, A. A.; Fu, B.; Patel, V.; Seo, B. M.; Sonoyama, W.; Zheng, J. J.; Baker, C. C.; Chen, W.; Ried, T.; Shi, S. Accumulated chromosomal instability in murine bone marrow mesenchymal stem cells leads to malignant transformation. Stem Cells 24:1095–1103; 2006.

30. Ng, F.; Boucher, S.; Koh, S.; Sastry, K. S.; Chase, L.; Lakshmipathy, U.; Choong, C.; Yang, Z.; Vemuri, M. C.; Rao, M. S.; Tanavde, V. PDGF, TGF-β, and FGF signaling is important for differentiation and growth of mesenchymal stem cells (MSCs): Transcriptional profiling can identify markers and signaling pathways important in differentiation of MSCs into adipogenic, chondrogenic, and osteogenic lineages. Blood 112:295–307; 2008.
31. Okamura, R. M.; Sigvardsson, M.; Galceran, J.; Verbeek, S.; Clevers, H.; Grosschedl, R. Redundant regulation of T cell differentiation and TCR alpha gene expression by the transcription factors LEF-1 and TCF-1. Immunity 8:11–20; 1998.
32. Park, J. Y.; Jeon, H. J.; Kim, T. Y.; Lee K. Y.; Park, K. S.; Lee, E. S.; Choi, J. M.; Park, C. G.; Jeon, S. H. Comparative analysis of mesenchymal stem cell surface marker expression for human dental mesenchymal stem cells. Regen. Med. 8:453–466; 2013.
33. Park, J. Y.; Jeon, S. H.; Choung, P. H. Efficacy of periodontal stem cell transplantation in the treatment of advanced periodontitis. Cell Transplant. 20:271–285; 2011.
34. Park, K. S.; Jeon, S. H.; Kim, S. E.; Bahk, Y. Y.; Holmen, S. L.; Williams, B. O.; Chung, K. C.; Surh, Y. J.; Choi, K. Y. APC inhibits ERK pathway activation and cellular proliferation induced by RAS. J. Cell Sci. 119:819 – 827; 2006.
35. Pittenger, M. F.; Mackay, A. M.; Beck, S. C. Jaiswal, R. K.; Douglas, R.; Mosca, J. D.; Moorman, M. A.; Simonetti, D. W.; Craig, S.; Marshak, D. R. Multilineage potential of adult human mesenchymal stem cells. Science 284:143–147; 1999.
36. Potapova, I. A.; Gaudette, G. R.; Brink, P. R.; Robinson, R. B.; Rosen, M. R.; Cohen, I. S.; Doronin, S. V. Mesenchymal stem cells support migration, extracellular matrix invasion, proliferation, and survival of endothelial cells in vitro. Stem Cells 25:1761–1768; 2007.
37. Reya, T.; Clevers, H. Wnt signalling in stem cells and cancer. Nature 434:843–850; 2005.
38. Rostovskaya, M.; Anastassiadis, K. Differential expression of surface markers in mouse bone marrow mesenchymal stromal cell subpopulations with distinct lineage commitment. PLoS One 7:e51221; 2012.
39. Sanchez-Ramos, J.; Song, S.; Cardozo-Pelaez, F.; Hazzi, C.; Stedeford, T.; Willing, A.; Freeman, T. B.; Saporta, S.; Janssen, W.; Patel, N.; Cooper, D. R.; Sanberg, P. R. Adult bone marrow stromal cells differentiate into neural cells in vitro. Exp. Neurol. 164:247–256; 2000.
40. Sasaki, M.; Abe, R.; Fujita, Y.; Ando, S.; Inokuma, D.; Shimizu, H. Mesenchymal stem cells are recruited into wounded skin and contribute to wound repair by transdifferentiation into multiple skin cell type. J. Immunol. 180:2581–2587; 2008.
41. Schinkothe, T.; Bloch, W.; Schmidt, A. In vitro secreting profile of human mesenchymal stem cells. Stem Cells Dev. 17:199–205; 2008.
42. Serakinci, N.; Guldberg, P.; Burns, J. S.; Abdallah, B.; Schrødder, H.; Jensen, T.; Kassem, M. Adult human mesenchymal stem cell as a target for neoplastic transformation. Oncogene 23:5095–5098; 2004.
43. Shi, S.; Gronthos, S. Perivascular niche of postnatal mesenchymal stem cells in human bone marrow and dental pulp. J. Bone Miner. Res. 18:696–704; 2003.
44. Staal, F. J.; Luis, T. C.; Tiemessen, M. M. WNT signalling in the immune system: WNT is spreading its wings. Nat. Rev. Immunol. 8:581–593; 2008.
45. Suniara, R. K.; Jenkinson, E .J.; Owen, J. J. An essential role for thymic mesenchyme in early T cell development. J. Exp. Med. 191:1051–1056; 2000.
46. Suzuki, A.; Raya, A.; Kawakami, Y.; Morita, M.; Matsui, T.; Nakashima, K.; Gage, F. H.; Rodríguez-Esteban, C.; Izpisúa Belmonte, J. C. Nanog binds to Smad1 and blocks bone morphogenetic protein-induced differentiation of embryonic stem cells. Proc. Natl. Acad. Sci. USA 103:10294–10299; 2006.
47. Takao, Y.; Yokota, T.; Koide, H. Beta-catenin up-regulates Nanog expression through interaction with Oct-3⁄4 in embryonic stem cells. Biochem. Biophys. Res. Commun. 353:699–705; 2007.
48. Tirode, F.; Laud-Duval, K.; Prieur, A.; Delorme, B.; Charbord, P.; Delattre O. Mesenchymal stem cell features of Ewing tumors. Cancer Cell 11:421–429; 2007.
49. Tolar, J.; Nauta, A. J.; Osborn, M. J.; Panoskaltsis Mortari, A.; McElmurry, R. T.; Bell, S.; Xia, L.; Zhou, N.; Riddle, M.; Schroeder, T. M.; Westendorf, J. J.; McIvor, R. S.; Hogendoorn, P. C.; Szuhai, K.; Oseth, L.; Hirsch, B.; Yant, S. R.; Kay, M. A.; Peister, A.; Prockop, D. J.; Fibbe, W. E.; Blazar, B. R. Sarcoma derived from cultured mesenchymal stem cells. Stem Cells 25:371–379; 2007.
50. Torensma, R.; Prins, H. J.; Schrama, E; Verwiel, E. T.; Martens, A. C.; Roelofs, H.; Jansen, B. J. The impact of cell source, culture methodology, culture location, and individual donors on gene expression profiles of bone marrow-derived and adipose-derived stromal cells. Stem Cells Dev. 22:1086–1096; 2012.
51. Wagner, W.; Wein, F.; Seckinger, A.; Frankhauser, M.; Wirkner, U.; Krause, U.; Blake, J.; Schwager, C.; Eckstein, V.; Ansorge, W.; Ho, A. D. Comparative characteristics of mesenchymal stem cells from human bone marrow, adipose tissue, and umbilical cord blood. Exp. Hematol. 33:1402–1416; 2005.
52. Wang, S.; Qu, X.; Zhao, R. C. Clinical applications of mesenchymal stem cells. J. Hematol. Oncol. 5:1–9; 2012.
53. Weissman, I. L. Stem cells: Units of development, units of regeneration, and units in evolution. Cell 100:157–168; 2000.
54. Wu, Y.; Chen, L.; Scott, P. G.; Tredget, E. E. Mesenchymal stem cells enhance wound healing through differentiation and angiogenesis. Stem Cells 25:2648–2659; 2007.
55. Yun, M. S.; Kim, S. E.; Jeon, S. H.; Lee, J. S.; Choi, K. Y. Both ERK and Wnt/beta-catenin pathways are involved in Wnt3a-induced proliferation. J. Cell Sci. 118:313–322; 2005.
56. Zhao, S.; Wehner, R.; Bornhauser, M.; Wassmuth, R.; Bachmann, M.; Schmitz, M. Immunomodulatory properties of mesenchymal stromal cells and their therapeutic consequences for immune-mediated disorders. Stem Cells Dev. 19:607–614; 2010.